

Effects of P and B addition on as-cast microstructure and homogenization parameter of Inconel 718 alloy

MIAO Zhu-jun¹, SHAN Ai-dang¹, WU Yuan-biao¹, LU Jun², HU Ying^{1,2}, LIU Jun-liang², SONG Hong-wei²

1. School of Materials Science and Engineering, Shanghai Jiao Tong University, Shanghai 200240, China;

2. Baosteel Research Institute, Baoshan Iron & Steel Co., Ltd., Shanghai 201900, China

Received 11 January 2011; accepted 8 October 2011

Abstract: The effects of phosphorus and boron addition on the as-cast microstructure and homogenization parameters of Inconel 718 were studied. The results indicate that the addition of phosphorus and boron promotes the formation of blocky Laves phase. Due to the strong segregation behavior of boron in the final residual liquid, a low melting B-bearing phase enriched in Nb, Mo and Cr is observed. According to the differential scanning calorimeter results and electron probe micro-analysis characterization, the solidification sequence of Inconel 718 with phosphorus and boron addition in best combination is determined as $L \rightarrow L+\gamma \rightarrow L+\gamma+MC \rightarrow L+\gamma+MC+Laves \rightarrow \gamma+MC+Laves+B\text{-bearing phase}$. Accordingly, the homogenization temperature is recommended to be adjusted at least 40 °C lower than that of standard Inconel 718 due to the existence of low melting B-bearing phase.

Key words: P; B; Inconel 718 alloy; solidification; microstructure; homogenization

1 Introduction

Inconel 718 is the most classical nickel-base superalloy so far, accounting for more than 50% of commercial superalloy productions in the world [1]. However, the service temperature of Inconel 718 is restricted to 650 °C owing to fast coarsening of the main strengthening phase (tetragonal DO_{22} -structure γ'' phase) after long period exposure to temperature above 650 °C [2, 3]. With the target at increasing the service temperature by 30–50 °C, a lot of attempts have been made and minor elements doping is regarded as the most economical way. Many researchers [4–8] demonstrated that the addition of minor element P at a little higher level (1.5×10^{-4} to 2.4×10^{-4}) could improve the stress rupture and creep properties significantly. Moreover, CAO and KENNEDY [9, 10] reported that strong interactions between P and B existed and much more beneficial effects could be obtained through P and B addition in combination. The best synergistic combination was $(2.1\text{--}2.4) \times 10^{-4}$ P+ $(1.00\text{--}1.2) \times 10^{-4}$ B [11, 12].

Much research has been undertaken on the stress

rupture and creep properties of Inconel 718, while less work was involved with the change of solidification behavior after P and B addition, especially for the investigation on best combination. In view of the industrial production, it is of great value to study the solidification process and homogenization treatment for producing large scale ingots in good quality. Hence, the main objective of this study is to analyze the as-cast microstructure and homogenization parameter of Inconel 718 with best P+B combination.

2 Experimental

By comparison, two ingots (10 kg each) with different P and B addition were prepared by remelting the same master Inconel 718 in a 20 kg vacuum induction furnace. The actual chemical compositions of the two alloys (virgin and A) were obtained through inductively coupled plasma analysis, as listed in Table 1. In order to speculate on the solidification sequence, differential scanning calorimeter (DSC) test was conducted on a Netzsch STA 449C instrument and the heating rate was controlled at 10 °C/min from 1000 to 1400 °C. The reaction temperatures of on-heating DSC

Table 1 Chemical compositions of alloys (mass fraction, %)

Alloy	C	N	P	B	Al	Cr
Virgin	0.05	0.006	0.004	0.001	0.52	19.5
A	0.05	0.006	0.024	0.010	0.52	19.5
Alloy	Mo	Ti	Nb	Fe	Ni	
Virgin	3.10	1.00	5.35	17.5	Bal.	
A	3.10	1.00	5.35	17.5	Bal.	

curves were determined by Netzsch Proteus Analysis software.

Microstructure analysis samples were cut from the longitudinal center of the two ingots. After standard metallographic procedures, samples were electrolytic etched with a solution of 10 mL HCl+30 mL HNO₃+50 mL C₃H₈O₃ at 6 V for 10 s. HITACHI S-4200 scanning electron microscope (SEM) with INCA energy dispersive spectrum (EDS) examination was used to characterize the microstructures. Mapping distribution was analyzed on a JEOL JXA-8500F thermal field emission electron probe micro-analysis (FE-EPMA), with TAP, PETH, LDE2H and LIF analysis crystals used.

3 Results and discussion

Figures 1 (a) and (c) show the microstructures of two ingots at the center. At lower magnification, similar dendrite structures are found and black areas are the inter-dendritic areas where segregation phases form in the last stage of solidification. Detailed microstructures

at higher magnification for both alloys are shown in Figs.1 (b) and (d). For virgin alloy, two kinds of morphology are observed in terms of Laves phase: eutectic Laves and blocky Laves. However, only blocky Laves phase exists in alloy A, and the size is relatively bigger than that in the virgin alloy, which suggests that P and B additions may promote the formation of blocky Laves phase. Apart from that, the MC-type carbides in both alloys exhibit common morphology in the vicinity of Laves phase.

Combined with the previous metallographic observations, DSC examinations were carried out to further investigate the difference between the virgin alloy and alloy A concerning the solidification behavior. DSC on-heating curve for the virgin alloy illustrated in Fig. 2 shows that melting takes place for three stages like other references recorded [13, 14]: the melting of eutectic Laves and blocky Laves (P-H2), followed by the melting of MC carbide (P-H3) and finally the melting of primary γ matrix (P-H4). Quite unlike the DSC on-heating curves obtained in the previous investigations [13–15], peak P-H1 is observed in alloy A besides the above three peaks, which evidently demonstrates the existence of another unknown low melting phase (temporarily named as P_s). The detailed peak temperatures on-heating curves are summarized in Table 2. Based upon the data, it is reasonable to conclude that the solidification reaction temperatures of alloy A are postponed due to the addition of P and B. Hence, the solidification sequence of alloy A can be determined

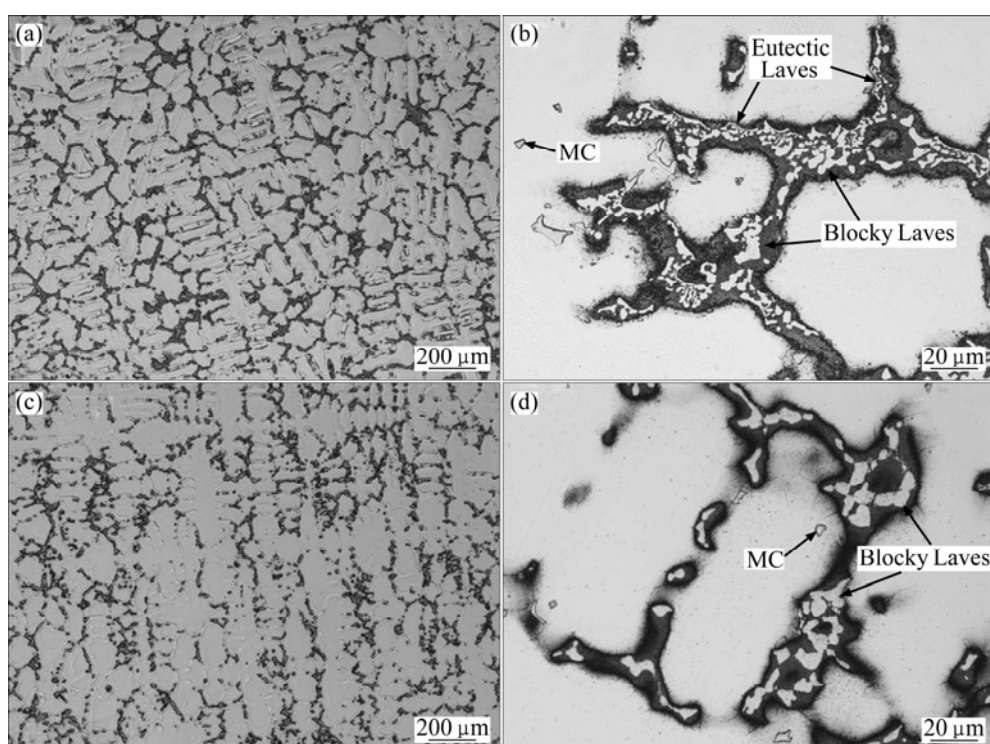


Fig. 1 Optical micrographs of as-cast microstructure in virgin alloy (a), (b) and alloy A (c), (d)

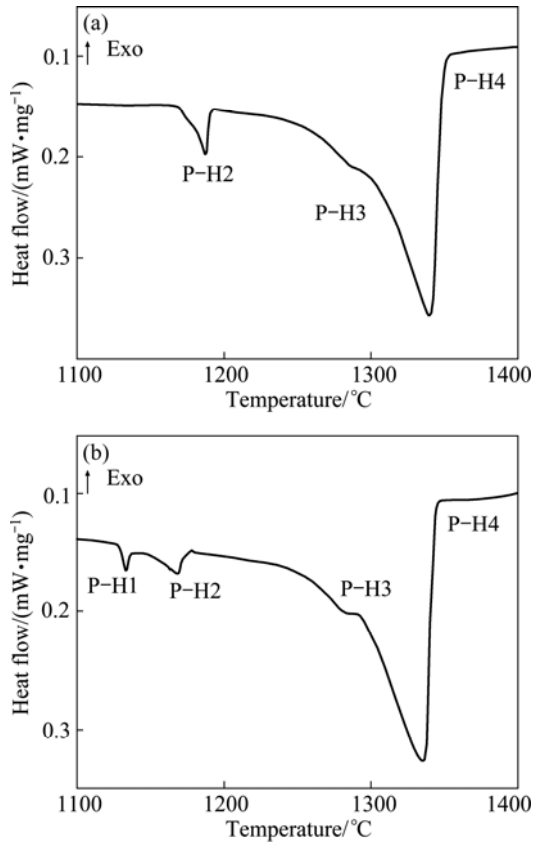


Fig. 2 Representative DSC on-heating curves for virgin alloy (a) and alloy A (b)

Table 2 Melting reaction peak temperatures in DSC on-heating curves shown in Fig. 2

Alloy	Peak temperature/°C			
	P-H1	P-H2	P-H3	P-H4
Virgin	Not detected	1187.8	1290.8	1339.8
A	1133.7	1169.2	1286.8	1335.2

preliminarily corresponding to the melting sequence of that as: $L \rightarrow L+\gamma \rightarrow L+\gamma+MC \rightarrow L+\gamma+MC+Laves \rightarrow \gamma+MC+Laves+P_s$.

As to the location where the unknown low melting phase (P_s) exists, inter-Laves phase region is the most likely according to the above analysis. In order to characterize this unknown low melting phase, FE-EPMA mapping distribution as well as EDS analysis was performed. Figure 3 shows the inter-Laves phase region at high magnification in alloy A and correspondent element distribution. Apart from the common phases such as γ and δ in the vicinity of Laves phase, one L-shape phase appears next to the Laves phase. When viewed in the perspective of elements distribution, it is clearly found that L-shape phase is enriched in Nb, Mo and B while depleted in Ni and P. Figure 4 and Table 3 show the difference of EDS profile between L-shape B-bearing phase and Laves phase in alloy A. High

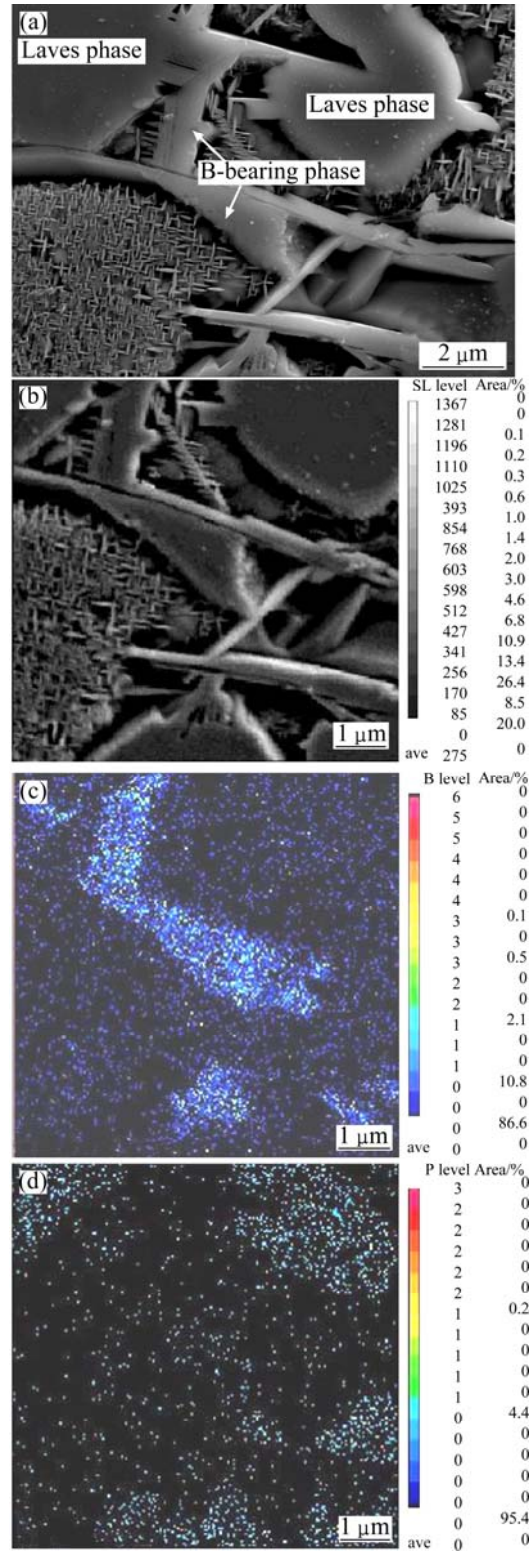


Fig. 3 Micrograph (a) and element distribution of B and P (b), (c), (d) in inter-Laves region

concentration of 35.6% Nb and 14.2% Mo (mass fraction) are found in the B-bearing phase. In the previous work, it was reported that B-bearing phases are enriched in Mo and Cr [16–18]. As known, Nb and Mo show close similarity in atomic radius and segregation behavior.

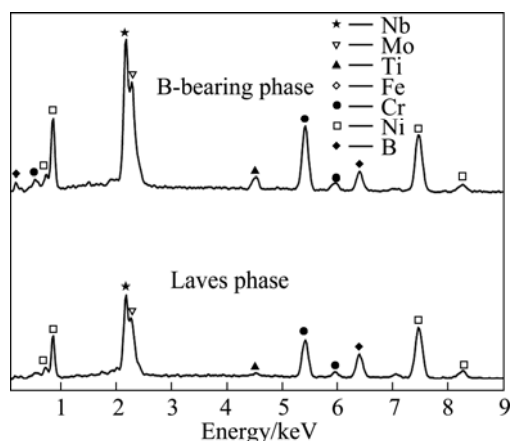


Fig. 4 EDS profiles of B-bearing phase and Laves phase in alloy A

Table 3 Measured compositions of Laves phase and B-bearing phase in alloy A (mass fraction, %)

Phase	w(Nb)/%	w(Mo)/%	w(Cr)/%	w(Ni)/%
Laves phase	31.11	8.33	12.97	34.54
B-bearing phase*	35.62	14.24	16.92	24.27
Phase	w(Fe)/%	w(Ti)/%	w(Al)/%	w(P)/%
Laves phase	10.84	0.84	0.20	1.17
B-bearing phase*	6.25	2.48	0.22	–

*Element B is not included because of equipment limitation

Therefore, Nb can replace Mo in the B-bearing phase. Furthermore, boron as a positive segregation element is also strongly enriched in the final residual melt, combining Nb and Mo to form B-bearing phase.

In consequence, the solidification sequence of alloy A can be modified as $L \rightarrow L+\gamma \rightarrow L+\gamma+MC \rightarrow L+\gamma+MC+Laves \rightarrow \gamma+MC+Laves+B\text{-bearing phase}$. It is also noted that little solubility of P in B-bearing phase and good solubility of P in Laves phase are seen in P-mapping. Simultaneously, little solubility of B in Laves phase is found in B-mapping. These two phenomena attribute to the fact that P and B cannot coexist in one phase.

Homogenization is a heat treatment of as-cast superalloy at high temperature for a long time to remove low melting phase and micro-segregation. Since homogenization is a diffusion-control process, the homogenization temperature is chosen as high as possible without reaching the incipient melting temperature (IMT) [19]. Typically, the homogenization temperature of standard Inconel 718 is in the range of 1170–1175 °C [20–21]. Hence, the homogenization parameters should be adjusted accordingly for Inconel 718 with best P+B combination. From the previous DSC data, the IMT of virgin alloy is 1176.9 °C. In contrast, the initial melting for alloy A takes place at 1129.2 °C. Here, metallographic method was applied to determine

the IMT in actual homogenization circumstance. In reference with DSC results, the samples were soaked at 1120, 1135, 1160, 1170 and 1185 °C for 30 min, respectively and then quenched in water.

Figure 5 shows the microstructure evolution of virgin alloy through different heating processes. Apparently, no change is discovered for Laves phase morphology after 1160 and 1170 °C heating process. When the holding temperature is raised to 1185 °C, the melting of Laves phase occurs and the melting pool forms instead. For alloy A, the initial melting takes place much earlier, as shown in Fig. 6. When the holding temperature is 1120 °C, the microstructure does not change. Once the holding temperature is increased to 1135 °C, the B-bearing phase that exists in the vicinity of Laves phase begins to melt. Subsequently, the melting of

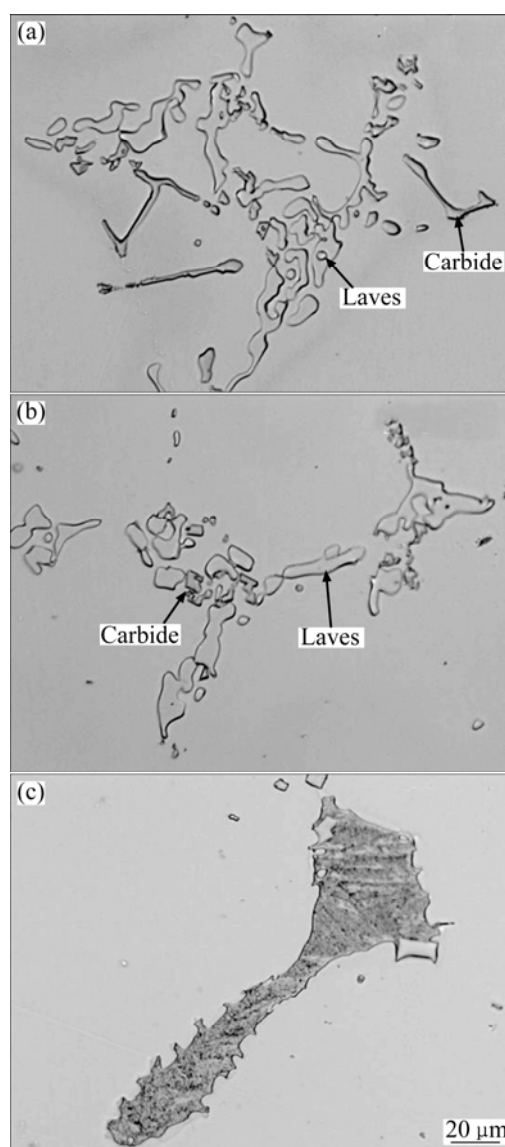


Fig. 5 OM images showing determination of incipient melting temperature of virgin alloy: (a) 1160 °C; (b) 1170 °C; (c) 1185 °C

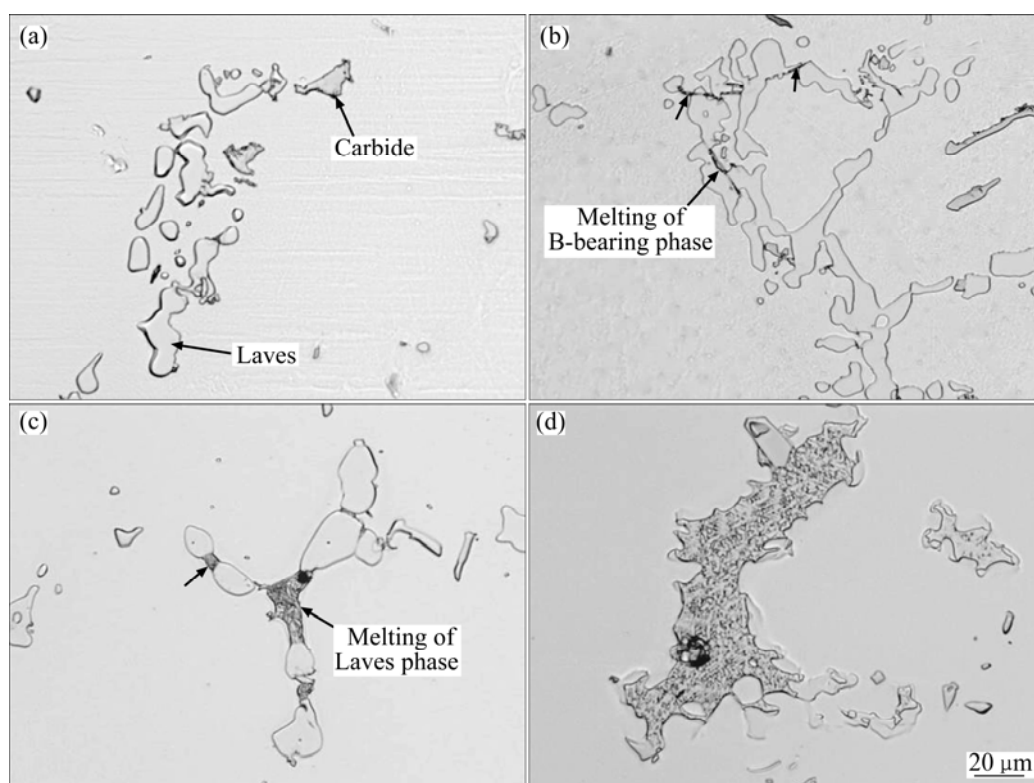


Fig. 6 OM images showing determination of incipient melting temperature of alloy A: (a) 1120 °C; (b) 1135 °C; (c) 1160 °C; (d) 1170 °C

Laves phase occurs at 1160 °C and the whole Laves phase becomes a melting pool at 1170 °C.

In the view of the above analysis, it is reasonable to conclude that the homogenization temperature of Inconel 718 with best P and B combination should be designed at least 40 °C lower than that of standard Inconel 718 owing to the existence of B-bearing phase.

4 Conclusions

1) Phosphorus and boron have strong effects on the as-cast microstructure of Inconel 718 and promote the formation of blocky Laves phase in particular.

2) B-bearing phase enriched in Nb, Mo and Cr is observed as a result of P and B addition in best combination.

3) The homogenization temperature of Inconel 718 with P and B addition is recommended to be adjusted at least 40 °C lower than that of standard Inconel 718 due to the existence of low melting B-bearing phase.

Acknowledgments

One of the authors MIAO Zhu-jun would like to thank Dr. SUN Wen-ru from Institute of Metal Research, Chinese Academy of Sciences for alloy preparation and useful discussions.

References

- [1] DECKER R. The evolution of wrought age-hardenable superalloys [J]. *JOM*, 2006, 58: 32–36.
- [2] OTT E, GROH J, SIZEK H. Metals affordability initiative: application of allvac alloy 718 Plus for aircraft engine static structural components [C]//LORIA E A. Proceedings of Superalloys 718, 625, 706 and Derivatives. PA, USA: TMS, 2005: 35–46.
- [3] SMITH G, PATEL S. The role of niobium in wrought precipitation-hardened nickel-base alloys [C]//LORIA E A. Proceedings of Superalloys 718, 625, 706 and Derivatives. PA, USA: TMS, 2005: 135–154.
- [4] LIU X, DONG J, TANG B, HU Y, XIE X. Investigation of the abnormal effects of phosphorus on mechanical properties of Inconel 718 superalloy [J]. *Materials Science and Engineering A*, 1999, 270: 190–196.
- [5] SONG H, GUO S, HU Z. Beneficial effect of phosphorus on the creep behavior of Inconel 718 [J]. *Scripta Materialia*, 1999, 41: 215–219.
- [6] LI N, SUN W, XU Y, GUO S, LU D, HU Z. Effect of P and B on the creep behavior of alloy 718 [J]. *Materials Letters*, 2006, 60: 2232–2235.
- [7] SUN W, GUO S, LEE J, PARK N, YOO Y, CHOE S, HU Z. Effect of phosphorus on the Ni₃Nb phase precipitation and the stress rupture properties in alloy 718 [J]. *Materials Science and Engineering A*, 1998, 247: 173–179.
- [8] GUO S, SUN W, LU D, HU Z. Effect of minor elements on microstructure and mechanical properties of Inconel 718 alloy [C]//LORIA E A. Proceedings of Superalloys 718, 625, 706 and Derivatives. PA, USA: TMS, 1997: 521–530.

- [9] CAO W, KENNEDY R. Effect and mechanism of phosphorus and boron on creep deformation of alloy 718 [C]//LORIA E A. Proceedings of Superalloys 718, 625, 706 and Derivatives. PA, USA: TMS, 1997: 511–520.
- [10] CAO W, KENNEDY R. New developments in wrought 718-type superalloys [J]. Acta Metallurgica Sinica, 2005, 18: 39–46.
- [11] HORTON J, McKAMEY C, MILLER M, CAO W, KENNEDY R. Microstructural characterization of superalloy 718 with boron and phosphorus additions [C]//LORIA E A. Proceedings of Superalloys 718, 625, 706 and Derivatives. PA, USA: TMS, 1997: 401–408.
- [12] McKAMEY C, CARMICHAEL C, CAO W, KENNEDY R. Creep properties of phosphorus + boron-modified alloy 718 [J]. Scripta Materialia, 1998, 38: 485–491.
- [13] KNOROVSK G, CIESLAK M, HEADLEY T, ROMIG A, HAMMETTER W. Inconel 718: A solidification diagram [J]. Metallurgical and Materials Transactions A, 1989, 20: 2149–2158.
- [14] CIESLAK M, HEADLEY T, KNOROVSK G, ROMIG A, KOLLIE T. A comparison of the solidification behavior of INCOLOY 909 and Inconel 718 [J]. Metallurgical and Materials Transactions A, 1990, 21: 479–488.
- [15] DUPONT J, NOTIS M, MARDER A, ROBINO C, MECHAEAL J. Solidification of Nb-bearing superalloys: Part I. Reaction sequences [J]. Metallurgical and Materials Transactions A, 1998, 29: 2785–2796.
- [16] WALSH J, KEAR B. Direct evidence for boron segregation to grain boundaries in a nickel-base alloy by secondary ion mass spectrometry [J]. Metallurgical and Materials Transactions A, 1975, 6: 226–229.
- [17] GAROSSHEN T, TILLMAN T, McCARTHY G. Effects of B, C, Zr on the structure and properties of a P/M nickel base superalloy [J]. Metallurgical and Materials Transactions A, 1987, 18: 69–77.
- [18] YAN B, ZHANG J, LOU L. Effect of boron additions on the microstructure and transverse properties of a directionally solidified superalloy [J]. Materials Science and Engineering: A, 2008, 474: 39–47.
- [19] FORBES JONES R, JACKMAN L. The structural evolution of superalloy ingots during hot working [J]. JOM, 1999, 51: 27–31.
- [20] LIANG X, ZHANG R, YANG Y, HAN Y. An investigation of the homogenization and deformation of alloy 718 ingots [C]//LORIA E A. Proceedings Superalloys 718, 625, 706 and Derivatives. PA, USA: TMS, 1994: 949–958.
- [21] MIAO Zhu-jun, SHAN Ai-dang, WU Yuan-biao, LU Jun, XU Wen-liang, SONG Hong-wen. Quantitative analysis of homogenization treatment of Inconel 718 superalloy [J]. Transactions of Nonferrous Metals and Society of China, 2011, 21(5): 1009–1017.

磷硼复合添加对 Inconel 718 合金铸态组织及均匀化处理参数的影响

缪竹骏¹, 单爱党¹, 吴元彪¹, 卢俊², 胡莹^{1,2}, 刘俊亮², 宋洪伟²

1. 上海交通大学 材料科学与工程学院, 上海 200240;
2. 宝山钢铁股份有限公司 宝钢研究院, 上海 201900

摘要: 研究磷硼复合添加对 Inconel 718 高温合金铸态组织及均匀化处理参数的影响。结果表明: 磷硼的加入促进块状 Laves 相的形成。由于硼在最后残余液相中大量富集, 形成一种富含 Nb、Mo 和 Cr 的含硼相。根据 DSC 和电子探针分析结果, 确定磷硼复合添加 Inconel 718 高温合金的凝固顺序为 $L \rightarrow L+\gamma \rightarrow L+\gamma+MC \rightarrow L+\gamma+MC+Laves \rightarrow \gamma+MC+Laves+含硼相$ 。由于低熔点含硼相的存在, 磷硼复合添加 Inconel 718 高温合金的均匀化处理温度应比标准 Inconel 718 合金低至少 40 °C。

关键词: 磷; 硼; Inconel 718 合金; 凝固; 微观组织; 均匀化处理

(Edited by FANG Jing-hua)